

A Study of a Wind Farm Power System

Preprint

E. Muljadi, Y. Wan, C.P. Butterfield,
and B. Parsons

*To be presented at the 21st American Society of
Mechanical Engineers Wind Energy Symposium
Reno, Nevada
January 14–17, 2002*



NREL

National Renewable Energy Laboratory

1617 Cole Boulevard
Golden, Colorado 80401-3393

NREL is a U.S. Department of Energy Laboratory
Operated by Midwest Research Institute • Battelle • Bechtel

Contract No. DE-AC36-99-GO10337

NOTICE

The submitted manuscript has been offered by an employee of the Midwest Research Institute (MRI), a contractor of the US Government under Contract No. DE-AC36-99GO10337. Accordingly, the US Government and MRI retain a nonexclusive royalty-free license to publish or reproduce the published form of this contribution, or allow others to do so, for US Government purposes.

This report was prepared as an account of work sponsored by an agency of the United States government. Neither the United States government nor any agency thereof, nor any of their employees, makes any warranty, express or implied, or assumes any legal liability or responsibility for the accuracy, completeness, or usefulness of any information, apparatus, product, or process disclosed, or represents that its use would not infringe privately owned rights. Reference herein to any specific commercial product, process, or service by trade name, trademark, manufacturer, or otherwise does not necessarily constitute or imply its endorsement, recommendation, or favoring by the United States government or any agency thereof. The views and opinions of authors expressed herein do not necessarily state or reflect those of the United States government or any agency thereof.

Available electronically at <http://www.osti.gov/bridge>

Available for a processing fee to U.S. Department of Energy
and its contractors, in paper, from:

U.S. Department of Energy
Office of Scientific and Technical Information
P.O. Box 62
Oak Ridge, TN 37831-0062
phone: 865.576.8401
fax: 865.576.5728
email: reports@adonis.osti.gov

Available for sale to the public, in paper, from:

U.S. Department of Commerce
National Technical Information Service
5285 Port Royal Road
Springfield, VA 22161
phone: 800.553.6847
fax: 703.605.6900
email: orders@ntis.fedworld.gov
online ordering: <http://www.ntis.gov/ordering.htm>



A STUDY OF A WIND FARM POWER SYSTEM

E. Muljadi

Y. Wan

C.P. Butterfield

B. Parsons

National Wind Technology Center
National Renewable Energy Laboratory
Golden, Colorado

ABSTRACT

A wind power system differs from a conventional power system. In a conventional power plant, the operator can control the plant's output. The output of a wind farm cannot be controlled because the output fluctuates with the wind. In this study, we investigated only the fixed-frequency induction generator, often used with wind turbines. We adopted the worst-case scenario and conducted a per-phase, per-turbine analysis. Our analysis showed a strong interaction among the wind farm, the utility grid, and the individual generator.

In this paper, we investigate the power-system interaction resulting from power variations at wind farms using steady-state analysis. We use the characteristic of a real windsite on a known weak grid. We present different types of capacitor compensations and use phasor diagrams to illustrate the characteristics of these compensations. The purpose of our study is to provide wind farm developers with some insights on wind farm power systems.

Key words: wind turbine, power system, wind farm, renewable energy, stability, voltage fluctuation, capacitor compensation, induction generator, reactive power compensation.

INTRODUCTION

In the early stages of wind energy development, the number of turbines is small and the locations of the farms are scattered. Thus the contribution of power from wind farms to the grid is negligible. As the size of a wind farm gets larger, the contribution of the power from the farm gets larger, and the interaction between wind farm and grid becomes more important to the operator and utility company. Many wind turbines use fixed-frequency induction generators. The induction generator is connected directly to the utility line. The power system's problems related to fixed-frequency wind turbines are more challenging to engineers than the variable-speed wind turbines, because there is minimum control that can be applied to fixed-frequency induction generators.

Figure 1 shows a cluster of wind turbines connected to a grid. The single-line diagram representing the system is shown on the same figure. The wind turbine is operated using a constant-frequency induction gen-

erator. Each generator is connected to a distribution transformer at the foundation of the wind turbine. The output from each wind turbine is connected to interconnection point to be called the *point of common coupling* (PCC). From the PCC, the output is connected to a transmission transformer, raised to a high voltage, and transmitted over the transmission line. At the end of transmission line, it is connected to the rest of a much larger grid (infinite bus). The impedance of the transformers and transmission lines are lumped together and is represented as Z_s .

While conventional power plants use synchronous generators, a wind farm power plant uses induction generators as the main generation. The behavior of the synchronous generator is very well known and has been investigated for more than a hundred years. Similarly, the behavior of the induction motor is widely known. Although considerable effort has been spent on developing induction motors, induction generators are not commonly used in conventional power plants.

In this study, we use the characteristics of the power system for a real wind farm connected to a known weak grid. The lines between the wind farm and the infinite bus may have several connections to feed small towns or loads along the way. We investigate how the voltage behaves at these connections when the wind speed

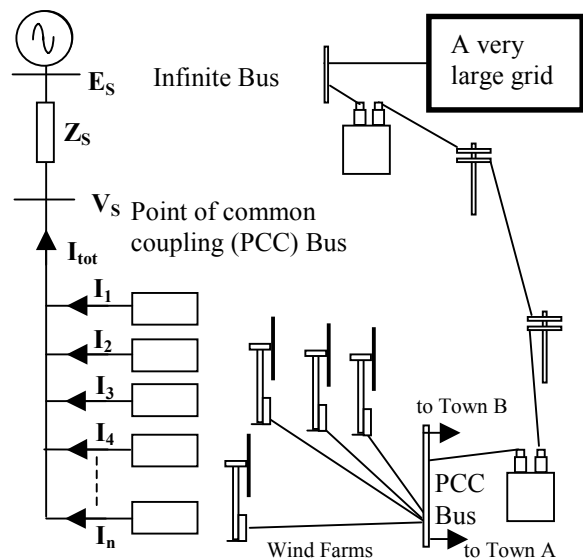


Figure 1. Multiple wind turbines feeding the grid

changes. The voltage variation at the PCC not only affects customers connected to the same point (Town A and Town B), but also affects the entire wind farm. Another important aspect of the investigation is the stability of the power system at the wind farm. It is shown in the next few sections that a strong correlation exists between the voltage variations and the stability of the systems. Instability can cause the whole wind farm to shut down.

Many publications have discussed hybrid power systems with diesel generators operating in parallel with wind turbines,^{1,2,3} however, wind farm power systems were considered less problematic than hybrid systems. Unfortunately, not all wind farms are connected to a stiff grid. Many areas with excellent wind resources are located in weak grid systems. Also, many wind farms increase their output by installing bigger and newer wind turbines.

While a dynamic simulation is an important tool in determining the stability of the wind farm power system,^{4,5,6} the big picture of a wind farm operation can be better understood from the basic characteristics of each component. Steady-state analysis is used to explain the behavior of a wind farm power system because it gives a broader spectrum in understanding the system interaction.

In the sections that follow, we first describe the components of a wind farm power system, including the wind turbine, induction generator, and parallel representation of wind turbines. Next, we discuss the per-phase, per-turbine equivalent circuit representing the entire power system, and then present different types of compensation. Finally we summarize the paper in the conclusion section.

COMPONENTS OF A WIND FARM POWER SYSTEM

Wind Turbine

The simple aerodynamic model commonly used to represent the turbine is based on power performance versus tip-speed ratio (C_p -TSR). The C_p -TSR characteristic of the turbine is derived from measured average output power and average wind speed. The aerodynamic power generated by the wind turbine is determined by the density of air, the radius of the blade, the performance coefficient at any instant, and the wind speed.

Figure 2 shows curves of aerodynamic power output for wind turbines at different rotor speeds. It is assumed that the wind turbine is stall-control operated at a constant frequency. The rotor speeds shown on the legend are the rotor rpm at the high-speed shaft (at the generator side). As can be expected, the peaks of available aerodynamic power increases as the rotor rpm is

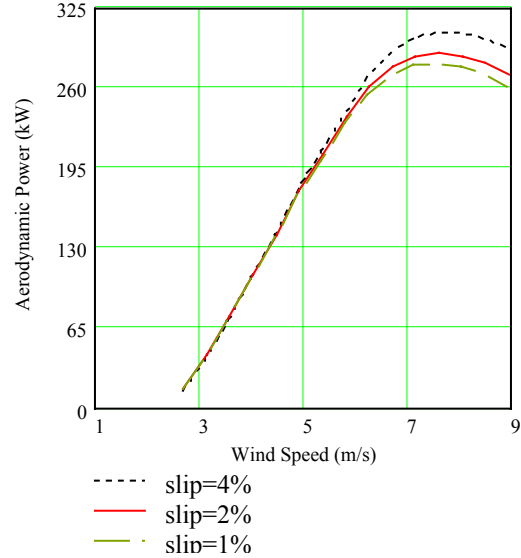


Figure 2. Aerodynamic power versus wind speed for different rotor rpm (stall control)

fixed at higher speeds. Thus, operation at high slip increases the aerodynamic power capability of the wind turbine. Once a runaway occurs for a stall-controlled wind turbine, the generator cannot regain control of the wind turbine. Some type of braking mechanism must be available to control the rotor speed.

Induction Generator

Figure 3 shows a typical power-speed characteristic of an induction machine as the operating slip varies from slip = 1 (motoring) to slip = -1 (generating). Assuming there are no losses in the induction generator, the power shown in Figure 3 is the power that must be driven by the wind turbine. Normal (stable) operating slips usually lie within a very narrow slip range (around $\pm 2\%$, bounded between P_{M-peak} and P_{G-peak} in Figure 3). The normal motoring region lies between 98% and 100% of synchronous speed, while the normal generat-

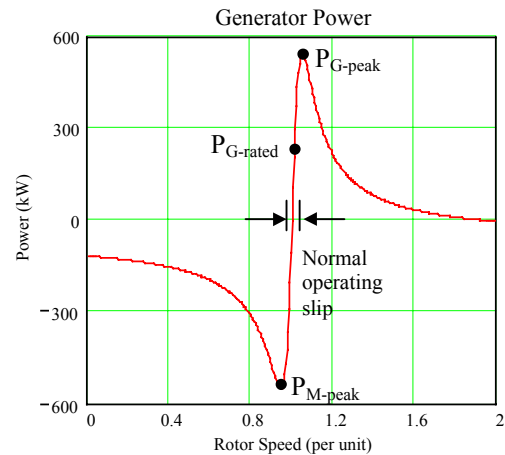


Figure 3. Generator power versus rotor speed

ing region lies between synchronous speed and about 102% of synchronous speed. Rated power is usually about 50% of peak power ($P_{G\text{-peak}}$).

The relationship between voltage and current of an induction machine varies as the slip changes from standstill to generating speed (above synchronous speed). At large slip, the stator current is much larger than in normal operating slip. As an example, at start-up (slip = 1), the stator current can reach up to 800% of the rated current. The magnitude and the phase angle of the stator current affects the voltage drop along the transmission line.

Parallel representation of wind turbines

As shown in Figure 1, a wind farm can be simplified as n parallel turbines. The following assumptions were made to simplify the analysis:

- The wind turbines are identical.
- Wind speeds at the wind farm are uniform, so that all wind turbines start at the same time.
- Each turbine runs at the same operating condition at all times; thus, the voltage, current, and power factor of each turbine are identical to the rest.
- The impedance of the line feeder between each turbine and the PCC is identical and negligible.

In practice, wind farms can be very large, and the locations of individual wind turbines can vary, as do the wind speeds at each wind turbine. The operating conditions of wind turbines can also be different with respect to each other. Thus, the assumptions above may lead to a pessimistic result or the worst-case scenario. Equations 1 through 6 are derived based on the sign and arrow convention of the voltages and currents shown in Figure 4. The variables printed in bold are phasors, and each equation can be expressed or illustrated by a phasor diagram. With only a single turbine operating, the terminal voltage at the PCC of the wind farm can be expressed as:

$$\mathbf{V}_S = \mathbf{E}_S - \mathbf{Z}_S \mathbf{I}_1 \quad [1]$$

If there are n identical turbines operating in parallel, the voltage equation can be expressed as:

$$\mathbf{V}_S = \mathbf{E}_S - \mathbf{Z}_S (\mathbf{I}_1 + \mathbf{I}_2 + \mathbf{I}_3 + \mathbf{I}_4 + \mathbf{I}_5 + \dots + \mathbf{I}_n) \quad [2]$$

With the assumption presented above, the currents in each branch are equal.

$$\mathbf{I}_1 = \mathbf{I}_2 = \mathbf{I}_3 = \mathbf{I}_4 = \mathbf{I}_5 = \dots = \mathbf{I}_n \quad [3]$$

The equation can be rewritten as:

$$\mathbf{V}_S = \mathbf{E}_S - \mathbf{Z}_S (n \mathbf{I}_1) \quad [4]$$

Or, if analyzed on a per-turbine basis, the equation becomes:

$$\mathbf{V}_S = \mathbf{E}_S - (\mathbf{Z}_S n) \mathbf{I}_1 \quad [5]$$

And the final solution is simplified as:

$$\mathbf{V}_S = \mathbf{E}_S - \mathbf{Z}_{S\text{NEW}} \mathbf{I}_1 \quad [6]$$

where: $\mathbf{Z}_{S\text{NEW}} = n \mathbf{Z}_S$.

Conducting our analysis on a per-turbine, per-phase basis enables us to understand the collective effects of wind turbine power generation in a wind farm environment. As shown by the equations above and in Figure 4, the number of turbines will change the characteristics of individual induction generators when the size of line impedance $\mathbf{Z}_{S\text{NEW}}$ grows larger as we add more turbines into the wind farm. For newly constructed wind farms, the grid system is usually computed for possible expansion in the future. In many places, however, a wind farm is connected to an existing grid. Although the transmission system in this grid is thermally capable of carrying the generated power, the system grid may be weak (\mathbf{Z}_S is large).

PER-PHASE, PER-TURBINE ANALYSIS

Figure 4 shows the per-phase, per-turbine equivalent circuit of an induction machine in a wind farm connected to the utility grid via a transmission line. The utility is represented by the infinite bus \mathbf{E}_S , and the reactance \mathbf{Z}_S represents line impedance and transformer impedance present between the induction machine and the infinite bus.

The number of wind turbines on-line determines the loading of the transmissions systems. Thus, it affects the voltage at the PCC. The characteristic of each induction generator connected to the same PCC will be affected. The number of wind turbines will appear as if the impedance \mathbf{Z}_S is multiplied by n , where n is the number of turbines operating at the same time. Thus, the more turbines are on-line, the weaker the grid appears to be (larger $\mathbf{Z}_{S\text{NEW}}$).

Figure 5 illustrates the loading effect on a certain transmission line. The impact of varying the slip of the induction generator and the impact of adding more turbines to the same line are shown. The normalized voltage at PCC for different numbers of turbines on-line also is shown. With only 10 wind turbines, it is obvious that the power system grid is stiff and the voltage does not change with slip. In the normal speed range be-

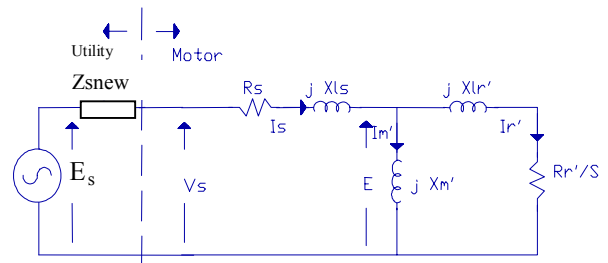


Figure 4. Equivalent circuit of an induction machine in per-phase, per-turbine analysis

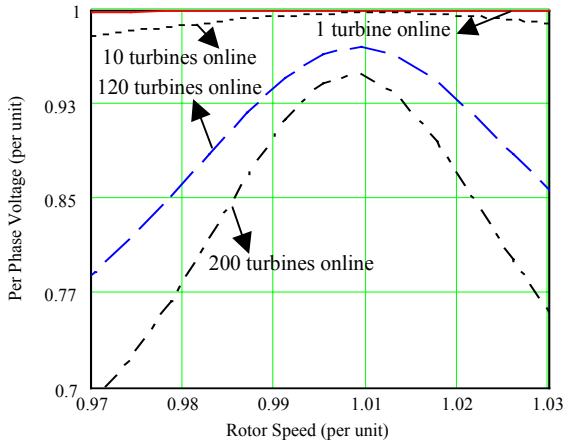


Figure 5. Per-phase voltage at PCC versus rotor speed

tween 0% slip (speed = 1.0 per unit or p.u.) and 2% slip (1.02 p.u.), the voltage variation at PCC is very small (about 1%). However, when the number of turbines is increased to 200, the voltage variation becomes larger. For example, for the same operating range, the voltage drops by as much as 15%.

The torque-speed characteristics of all individual wind turbines are identical, and the torque-speed characteristic shrinks as more turbines are connected on-line. To illustrate the effect of the number of turbines on torque capability, consider the torque-speed characteristic shown in Figure 6. The wind farm consists of wind turbines rated at 275 kilowatts each. Each wind turbine has an induction machine as the generator. Figure 6 shows that, with 10 wind turbines on-line, the torque-speed characteristic for an individual induction generator is barely changed. The resulting torque-speed characteristic of the individual induction generator is degraded dramatically as the number of turbines on-line

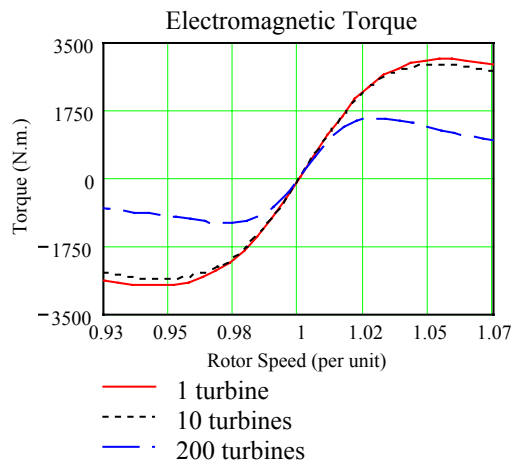


Figure 6. Torque-speed characteristic of individual induction machine

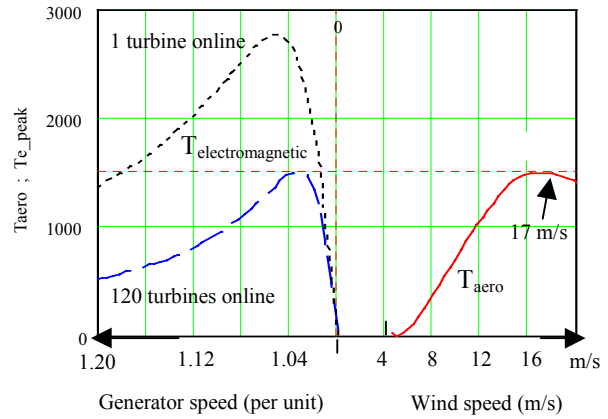


Figure 7. Peak electromagnetic torque and aerodynamic torque comparison

is increased to 200. Thus, there is a good chance that the aerodynamic power of the wind turbine will overpower the induction generator and the wind turbine will go into a runaway condition if nothing is done to control it. At the same time, the winding of the generator will be overheated and the voltage will collapse due to operation in a high-slip region.

This is illustrated in Figure 7, two-dimensional graph used to describe a three-dimensional problem. The vertical axis is used to represent the torque (electromagnetic torque and aerodynamic torque). The right-hand side of graph is used to represent the aerodynamic peak torque versus wind speed. It is shown that aerodynamic torque varies with the wind speed; it reaches its peak at 17 m/s. The left-hand side of the graph is used to represent the electromagnetic torque of the generator versus the wind speed for two different number of wind turbines on-line. It also shows that the peak of electromagnetic torque of the induction generator (the left-hand-side curve) shrinks as the number of turbines on-line is increased. By comparing the left-hand-side and the right-hand-side, it is shown that the electromagnetic peak torque drops below the peak of the aerodynamic torque when the number of turbines on-line is above 120. This is the operating point where instability occurs, thus the wind turbine is in a runaway condition. The slip at maximum electromagnetic torque is shown to be about 3%. The corresponding voltage at this point of instability can be referred to Figure 5, where it is shown that for 120 turbines online, at 3% slip (slip at peak torque), the voltage drops as much as 14% to 0.86 per unit. Thus in a way, the voltage drop indicates how close the operation of a wind turbine to the run-away condition. If the wind turbines lower voltage limit is set to 90% or higher, the runaway condition will not happen, because the wind turbine is taken off line before runaway condition occurs.

In the next few sections, the voltage profile at PCC and the stability of the induction generator will be discussed for different types of capacitor compensation. The contribution of each turbine to the total current in the transmission line will also be presented. The stability will be measured against an uncompensated system based on Figure 7, i.e., comparing the peak electromagnetic torque to the peak aerodynamic torque. In the real wind farm, the worst-case scenario may seldom occur, however, this pessimistic approach is a good measure of how close the operation of the wind farm is to the instability. The phasor diagrams presented are based on rated speed at -2% slip.

PARALLEL COMPENSATION

Parallel compensation is a common practice in wind turbine generation to improve the power factor of each turbine. Some wind turbines use more than one value of capacitor at their terminals to compensate reactive power for different wind speed. The advantage of an improved power factor is the reduction in total current, which, in turn, reduces transmission loss and improves voltage regulation. As an illustration, Figure 8 shows a per-phase, per-turbine equivalent circuit diagram of a wind turbine power plant compensated with a parallel capacitor at each turbine.

Note that although the circuit representing an induction machine is simplified as an impedance consisting of R_{IM} and X_{IM} , the actual calculations are based on a complete equivalent circuit. Typically, the current direction assumes the induction machine operates in motoring mode. The total current I_S is the sum of the wind turbine current I_M and the capacitor current I_C .

Based on the equivalent circuit diagram shown in Figure 8, the voltage and current equations can be written as:

$$E_S = V_S + n(R_S + jX_S)I_S \quad [7]$$

$$I_S = I_{IM} + I_C \quad [8]$$

The phasor diagram of voltages and currents for parallel compensation are shown in Figure 9. In Figure 9a, the phasor diagrams of an uncompensated system are

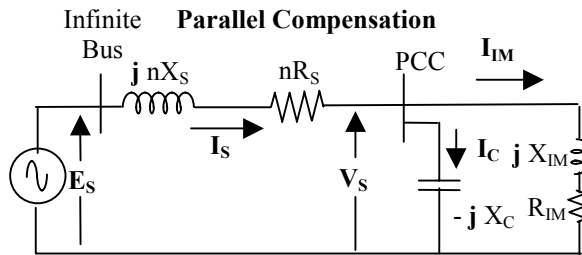


Figure 8. Per-turbine, per-phase equivalent circuit of an induction machine (simplified) in a wind farm with n turbines

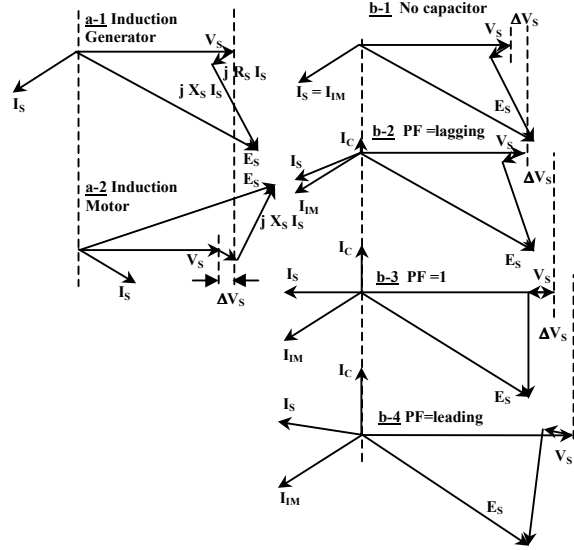


Figure 9. Phasor diagram of voltages and currents in a parallel compensated induction generator

presented. The phasor diagrams of voltage and current for motor operation and generator operations are shown.

In Figure 9b, the phasor diagrams for generating mode are presented for different sizes of capacitor compensation. Different capacitor sizes are shown on the phasor diagrams by the changes of the magnitude of capacitive currents I_C . Different sizes of capacitor current change the total current I_S , which effectively change the level of compensation. Figure 9b-1 is the phasor diagram of voltages and currents without compensation. The uncompensated system is used as the baseline. In Figure 9b-2, the capacitor compensation is small. There is a small increment ΔV_S of the magnitude of terminal voltage V_S . In Figure 9b-3, the compensation is adjusted to generate unity power factor output current by increasing the capacitor current I_C . Another increment in terminal voltage is shown. In this case, the terminal voltage is very close to the infinite bus voltage. Finally, in Figure 9b-4, the compensation is adjusted to generate a leading power factor. As a result, the terminal voltage V_S is higher than the infinite bus voltage E_S . Figure 9b shows that the terminal voltage is higher than the infinite bus voltage only at leading power factor, while the terminal voltage is lower than the infinite bus voltage at lagging power factor. Note that the phasor diagrams are calculated at one slip only (i.e., -2%).

For a reliable power transmission, the voltage variation should not be more than $\pm 10\%$ ⁷. Figure 10a shows that the terminal voltage drops below 90% when the system is not compensated. With parallel compensation of 800 μF and 1600 μF , the voltage V_S can be raised within the limit. Parallel compensation relies on

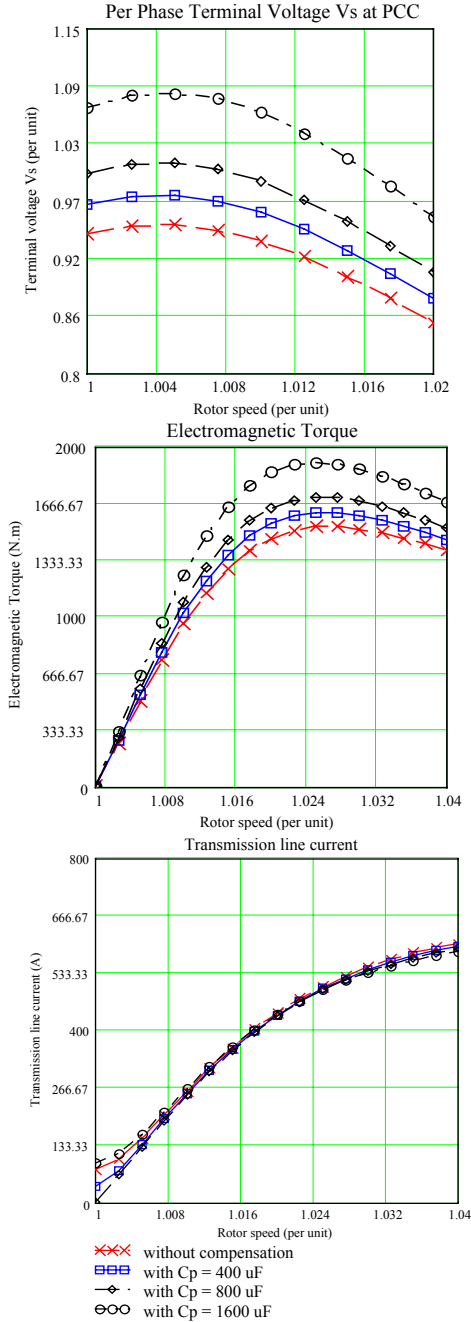


Figure 10. Parallel compensation with 200 turbines on-line
 a) Terminal voltage at PCC
 b) Electromagnetic torque
 c) Transmission line current (per turbine)

the reactive power generated by the capacitors in parallel with the induction generator. For a fixed parallel capacitor, the reactive power output of the capacitor is proportional to the square of the voltage across the capacitor. The reactive power required by induction machine varies with the operating slip. Thus, with a fixed

parallel capacitor, the voltage correction varies with the slip of the induction generator and the number of turbines on-line. In Figure 10a, the voltage at PCC is shown for different sizes of parallel capacitor compensation.

As shown in Figure 10a, the voltage is shown to improve as the parallel capacitor is increased. At 1600 uF, the voltage profile at PCC lies within 13% variation. The voltage improvement comes from an improved power factor after the capacitor is installed. In Figure 10b, the torque speed characteristic is shown to shift upward due to the available voltage at PCC increases by the additional capacitor. The wind turbine is improved with the installation of a parallel capacitor. As shown in Figure 7, the electromagnetic torque is overpowered by aerodynamic torque at 120 turbines for a system without capacitor compensation. With parallel capacitor compensation, the peak of generator torque is increased significantly. The line current per turbine shows a noticeable reduction at lower rotor speed (low slip operation) with parallel capacitor. At 200 turbines on-line, the parallel capacitor must be sized at least to 1600 uF per phase per turbine. This size of compensation enables the wind turbine to operate at PCC voltage within the limit, and the peak of generator torque is above the peak of aerodynamic torque shown in Figure 7.

To keep the terminal voltage constant, it is necessary to adjust the size of reactive power generated by the capacitor to follow the fluctuation in output power and to compensate for different number of turbines on-line. Different sizes of capacitors or a Static VAR Compensator (SVC) can be used where the reactive power can be adjusted continuously at a different slip or power level. Ideally, a small-sized capacitor can be used during low wind speed to raise the voltage to an appropriate level, and a larger capacitor can be used at a high wind speed region to raise the voltage and the electromagnetic torque above the peak of aerodynamic torque. However, even with a constant 1600-uF capacitor, the voltage V_s is still within reasonable range.

In the example above, it is shown that an additional 90 turbines can be installed for the same transmission line (assuming that the thermal limit and other transmission limit is not reached). Without parallel compensation, only 120 turbines can be installed.

SERIES COMPENSATION

In series compensation, the series capacitor is installed in series with the transmission line to compensate the transmission line. The size of the capacitor is chosen to compensate for the line impedance, i.e., to reduce the effective reactance in the line impedance. The voltage across a series capacitor has a 180° phase shift with respect to the voltage drop across the line

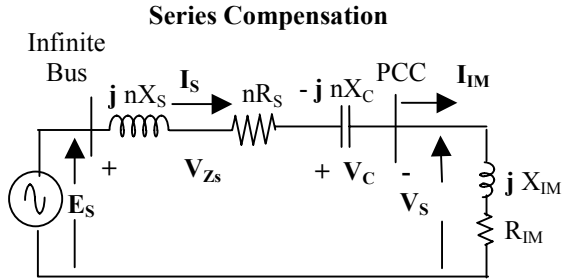


Figure 11. Series compensation of an induction machine (simplified) in a wind farm with n turbines

reactance X_s . Thus, the voltage across series capacitor (V_C) will be used to counteract the voltage drop across line impedance V_{ZS} . Series capacitors are often used to improve the power transfer capability of transmission lines.⁸ Variable series capacitance are often implemented by using thyristor control series (TCSC).

Figure 11 shows a per-phase, per-turbine equivalent circuit of a series-compensated system. Note that although the circuit is simplified, the actual calculations used to draw phasor diagrams are based on the complete circuit.

The equations based on voltages across the circuit's component can be written as:

$$E_s = V_s + V_{ZS} + V_C \quad [9]$$

$$V_{ZS} + V_C = n(R_s + j X_s) I_s - j n X_c I_s \quad [10]$$

The phasor diagrams shown in Figure 12 represent the voltages and current in a series compensation for different sizes of capacitor. With capacitor compensation, a small size of AC capacitor corresponds to a high reactance. In Figure 12a, the capacitor is sized such that the capacitive reactance of the capacitor compensates 75% of line reactance ($X_c = 0.75 X_s$). The re-

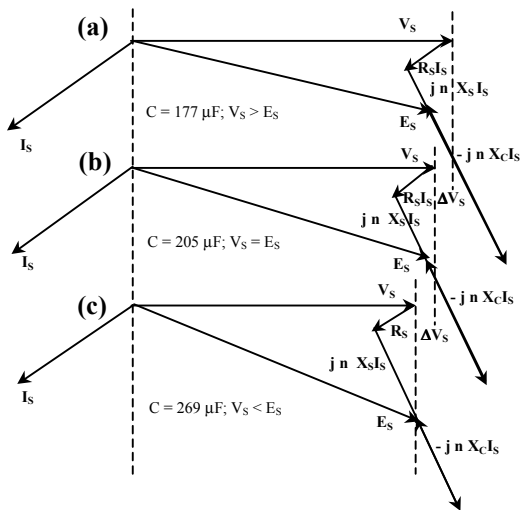


Figure 12. Phasor diagram of voltage and current for series compensation with different sizes of capacitors

sulting terminal voltage is higher than the infinite bus voltage ($V_s > E_s$). In Figure 12b, the capacitor is sized such that the terminal voltage is equal to the infinite bus voltage ($V_s = E_s$). As it turns out, the required capaci-

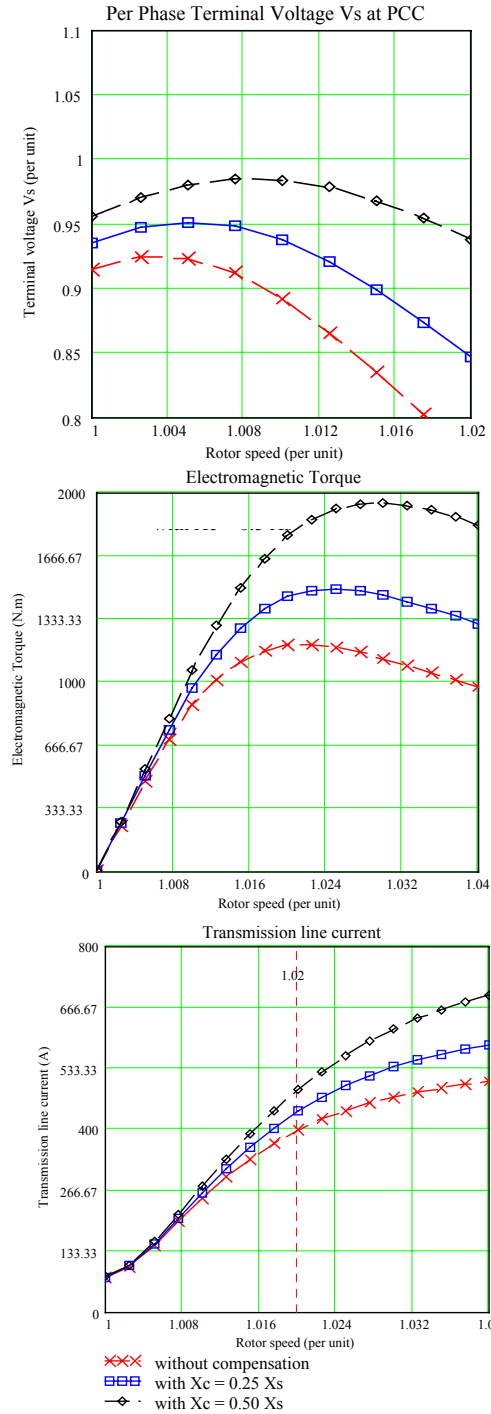


Figure 13. Series compensated with 300 turbines on-line
 a) Terminal voltage at PCC
 b) Electromagnetic torque
 c) Transmission-line current (per turbine)

tive reactance is 65% of the line reactance ($X_c = 0.65 X_s$). In Figure 12c, the capacitor is sized such that the capacitive reactance compensates 25% of the inductive reactance of the line impedance ($X_c = 0.25 X_s$). In this case, the terminal voltage is lower than the infinite bus voltage ($V_s < E_s$).

The terminal voltage at the PCC is shown in Figure 13a for series compensation. With series compensation, the number of turbines on-line can be increased up to 300. The voltage is within the 5% variation for ($X_c = 0.5 X_s$). When the size of the series capacitor is adjusted as such, the resulting $X_c = 0.5 X_s$. The resulting torque characteristic of the generator is illustrated in Figure 13b. It is shown that with $X_c = 0.5 X_s$, the electromagnetic torque of the generator can overcome the aerodynamic torque of the wind turbine (peak at 1875 Nm) as shown in Figure 7. Without compensation or insufficient compensation, the generator torque cannot overcome the aerodynamic torque and the system is in an unstable condition if the number of turbines on-line is increased to 300. The stator current in each turbine can be illustrated in Figure 13c. It is shown that although compensation improves the voltage profile and the torque profile of the generator, there is an increase on the stator current in comparison to the uncompensated system in the same situation (300 turbines on-line). Parallel compensation improves the effective power factor of the wind farm seen from the PCC, thus reducing the transmission line current and the corresponding losses. Series compensation reduces the voltage drop across the transmission line, thus improving the electromagnetic torque of the induction generator. The effective power factor of the wind farm is not affected by series compensation.

In a parallel compensation, the level of compensation decreases if the voltage across the capacitor decreases. On the other hand, in a series compensation, the level of compensation increases with the increase of the line current. It is necessary to investigate the variation of terminal voltage at different slip and with different number of turbines on-line to determine the range of voltage on the PCC at different conditions.

PARALLEL AND SERIES COMBINATION

It is apparent that we can take advantage of both parallel and series compensation of an AC capacitor. In a parallel compensation, the capacitor is used to compensate the individual induction generator. In series compensation, the capacitor is used to compensate the line impedance.

In this section, it is assumed that parallel compensation is used to compensate the basic need of reactive power of the induction generator. As shown in Equation 13 and Figure 15, each induction generator is compensated by a small parallel capacitor sized to compensate some portion of the reactive power needed by the in-

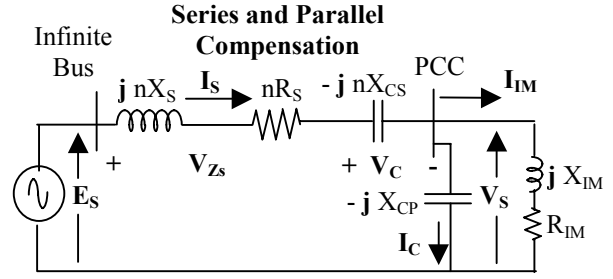


Figure 14. Series and parallel compensation of an induction machine (simplified)

duction generator. As the induction generator is driven by fluctuating wind speed, the overall power factor of the wind farm will be improved by the parallel capacitor attached to each turbine. The voltage drop across the line impedance will also be improved due to an overall better power factor of the wind farm. The series compensation used in series with the line impedance will appear as if the effective line reactance ($X_s - X_c$) is smaller, thus the whole grid will appear to be stiffer. Equations 11 and 12 show that the terminal voltage at PCC (V_s) can be regulated better because of partial cancellation of voltage drop across transmission V_{ZS} by series capacitor voltage V_C .

The equations for parallel and series combination can be written as:

$$E_s = V_s + V_{ZS} + V_C \quad [11]$$

$$V_{ZS} + V_C = n (R_s + j X_s) I_s - j n X_c I_s \quad [12]$$

$$I_s = I_{IM} + I_C \quad [13]$$

Figure 14 shows the per-turbine, per-phase equivalent circuit of a wind turbine connected to an infinite bus. The current flowing in the line impedance will have a less reactive component due to parallel capacitor C_p , while the effective voltage drop across line impedance

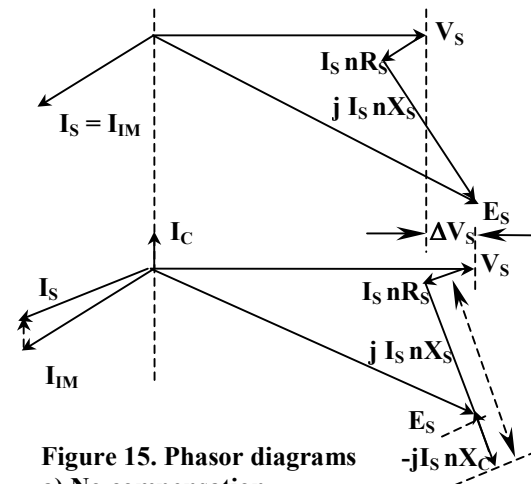


Figure 15. Phasor diagrams
a) No compensation
b) Parallel-series compensation

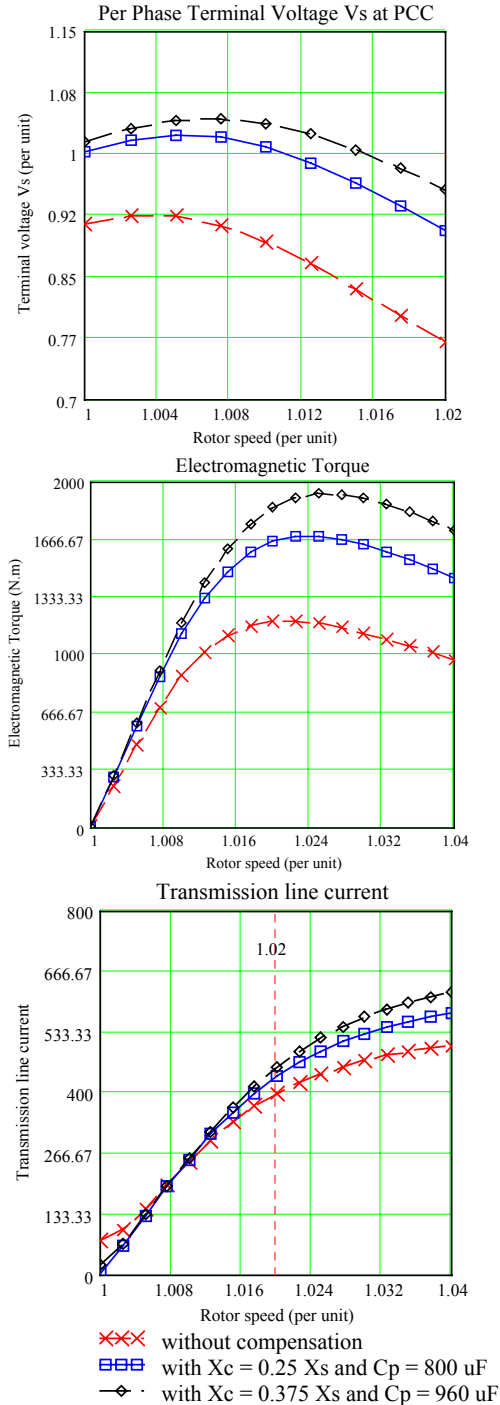


Figure 16. Parallel and series combination with 300 turbines on-line

- Terminal voltage at PCC
- Electromagnetic torque
- Stator current at each generator

(from one end to another) will be reduced by series capacitor C_s . The overall result will be an improvement

in the voltage fluctuation on the PCC and lower losses on the transmission line.

Figure 15 shows the phasor diagram of voltages and currents. Figure 15a shows a phasor diagram of the system before the compensation is applied. Figure 15b shows the phasor diagram of the system after the improvement is applied. In Figure 15a, the line current I_s is shown to be more in quadrature with the terminal voltage V_s and the voltage drop $I_s X_s$ is significantly large. The fact that I_s is more quadrature with respect to the terminal voltage V_s can only make the effect of large $I_s X_s$ voltage drop cause even lower-voltage V_s . After the compensation, the capacitor current I_C shifts the generator current I_{IM} upward so that the resulting line current I_s is shown to be significantly lower and has a better power factor. The impact of voltage-drop $I_s X_s$ is opposed by the voltage-drop across the capacitor $I_s X_c$. The overall improvement of parallel and series capacitor compensations is a narrower terminal voltage variation V_s .

Figure 16a illustrates the variation of terminal voltage as the speed or slip increases (a variation of 8%). The figure shows a significant voltage improvement for the system with capacitor compensations. A combination of $X_c = 50\% X_s$ and parallel capacitor of 960 μF gives a very good voltage profile at PCC, at the same time improving the torque speed characteristics (see Figure 16b). It is shown that at 2% slip, the terminal voltage of the compensated generator drops to about 0.95 per unit. With $X_c = 60\% X_s$, the terminal voltage will rise somewhat above the per unit voltage in the lower rotor speed. From Figure 16, it appears that a combination of $X_c = 0.375 X_s$ and $C_p = 960 \mu F$ per turbine will give the best result for normal operating range (slip = 0 to -2%). The generator torque is capable of holding the aerodynamic torque, and the reactive power required by the induction generator is compensated by the parallel capacitor, while the transmission line impedance is compensated by the series capacitor. As shown in Figure 16c and Figure 13c, a comparison between the stator current for series compensation and parallel-series compensation shows that the transmission line current is reduced significantly.

INPUT DATA USED

The input data used to compute and draw the phasor diagrams and the graph are based on the data presented in the table below.

TABLE 1. Input Data	
I. Induction Machine Data: (Y-connected)	
Stator Resistance	$R_s = 0.01027 \text{ ohm}$
Rotor Resistance	$R_r' = 0.01027 \text{ ohm}$
Stator Leakage	$X_{ls} = 0.1 \text{ ohm}$
Rotor Leakage	$X_{lr}' = 0.1 \text{ ohm}$

Magnetizing Reactance	$X_m = 3.3 \text{ ohm}$
Number of Poles	4
Rotor rpm	1800 at 0% slip
Frequency	60 Hz
Rated rpm HSS/LSS	1822 /53 rpm
Rated Power	275 kW
V_{LL}	480 volts
II. Transmission Line Data:	
66-kV base	480-V base
$X_s = 19.86 \text{ ohms}$	$X_s = 1.050 \times 10^{-3} \text{ ohms}$
$R_s = 5.23 \text{ ohms}$	$R_s = 2.766 \times 10^{-4} \text{ ohms}$
III. Operation Data	
Number of turbines= 300	$C_s = 177-269 \text{ uF at } 66\text{kV}$
Operating slip = - 2%	$C_p = 800\text{uF at } 480 \text{ V in Y}$

CONCLUSION

In this paper, we assumed the worst-case scenario for a wind farm, i.e., each wind turbine operates at exactly the same operating point throughout the entire farm. In reality, the wind farm usually covers a large area and the wind speed within the farm is not uniform. Thus the actual situation is usually better than the worst-case scenario. Based on a per-turbine analysis, we showed the following:

- Under per-phase, per-turbine conditions, having n turbines on-line has the same effect as having one turbine connected to an infinite bus via $n Z_s$ line impedance.
- As the number of turbine online increases, the available voltage at the point of common coupling is lower, and the torque-speed characteristic of the induction generator shrinks.
- We compare voltage profile at PCC, and the torque characteristic and the stator current at each turbine for different types of compensation.
- When the number of turbines on-line increases, the available voltage at PCC drops (due to high loading of the transmission system) and the torque-speed characteristic of the generator shrinks. As the margin of instability decreases, at one point, the wind turbine aerodynamic torque can overpower the generator torque and the operating slip increases further. At higher slip operation, the aerodynamic torque available increases. If no outside intervention (pitch control or mechanical brake) is taken, a runaway condition can occur.
- Capacitor compensation can help to boost the voltage at the PCC, thus improving the torque-speed capability of an individual induction generator.

- Ideal parallel compensation requires a variable reactive power as the output power and power factor fluctuates. A Static VAR Compensator can be used to provide parallel compensation with fluctuating reactive power needed.
- Series compensation can be used to offset the voltage drop across line impedance X_s . The size of the capacitance can be computed given the required compensation. TSCS can be considered to provide an adjustable series capacitor compensation.
- A combination of parallel and series compensation can be used to improve the overall system. With the correct choice of capacitor sizes, fixed capacitors can be used for both series and parallel compensation.
- We recommend that, during the wind farm design process, the characteristics of the induction generator be considered. The future expansion of the wind farm should also be taken into account.

ACKNOWLEDGEMENTS

The authors wish to thank Southern California Edison, especially Bob Yinger, for valuable discussions during the development of this project. We also wish to thank Demy Bucaneg and Tom Wilkins from Enron Wind. This work was supported by the U.S. Department of Energy.

REFERENCES

1. W.Q. Jeffries, Analysis and Modeling of Wind/Diesel Systems Without Storage, Ph.D. Thesis, Department of Mechanical Engineering, University of Massachusetts, 1994.
2. M.P. Papadopoulos, et al., Penetration of Wind Turbines in Islands with Diesel Power Stations, Proc. EWEC 1988, pp. 512-517, 1988.
3. J.T.G. Pierik, and De Bonte, Quasi Steady State Simulation of Autonomous Wind Diesel Systems (Status Report), Report No. ECN-85-091, Netherlands Energy Research Foundation, Petten, May 1985.
4. K. Uhlen, and O. Skarstein, A Short Term Dynamic Simulation Model for Wind/Diesel Systems, Proc. 10 BWEA Conference, pp. 239-242, 1988.
5. P.M. Anderson, A. Bose, Stability Simulation on Wind Turbine Systems, IEEE Transactions on Power Apparatus and Systems, Vol. PAS-102, No. 12, December 1983, pp. 3791-3795.
6. E.N. Hinrichsen, P.J. Nolan, Dynamic of Single and Multi Unit Wind Energy Conversion Plants Supplying Electric Utility Systems, OE/ET/20466 - 78/1 Report.
7. R. Grunbaum, B. Halvarsson, A. Wilk-Wilczynski, FACTS and HVDC Light for Power System Inter-

connections, presented at Power Delivery Conference, Madrid, Spain, September 1999.

8. Mid-Continent Area Power Pool (MAPP), Regional Reliability Handbook, MAPP, St. Paul, Mn. 1999.

REPORT DOCUMENTATION PAGE			Form Approved OMB NO. 0704-0188
Public reporting burden for this collection of information is estimated to average 1 hour per response, including the time for reviewing instructions, searching existing data sources, gathering and maintaining the data needed, and completing and reviewing the collection of information. Send comments regarding this burden estimate or any other aspect of this collection of information, including suggestions for reducing this burden, to Washington Headquarters Services, Directorate for Information Operations and Reports, 1215 Jefferson Davis Highway, Suite 1204, Arlington, VA 22202-4302, and to the Office of Management and Budget, Paperwork Reduction Project (0704-0188), Washington, DC 20503.			
1. AGENCY USE ONLY (Leave blank)	2. REPORT DATE January 2002	3. REPORT TYPE AND DATES COVERED Conference Paper	
4. TITLE AND SUBTITLE A Study of a Wind Farm Power System		5. FUNDING NUMBERS WER1.3010	
6. AUTHOR(S) E. Muljadi, Y. Wan, C.P. Butterfield, B. Parsons			
7. PERFORMING ORGANIZATION NAME(S) AND ADDRESS(ES)		8. PERFORMING ORGANIZATION REPORT NUMBER	
9. SPONSORING/MONITORING AGENCY NAME(S) AND ADDRESS(ES) National Renewable Energy Laboratory 1617 Cole Blvd. Golden, CO 80401-3393		10. SPONSORING/MONITORING AGENCY REPORT NUMBER NREL/CP-500-30814	
11. SUPPLEMENTARY NOTES NREL Technical Monitor: E. Muljadi			
12a. DISTRIBUTION/AVAILABILITY STATEMENT National Technical Information Service U.S. Department of Commerce 5285 Port Royal Road Springfield, VA 22161		12b. DISTRIBUTION CODE	
13. ABSTRACT (Maximum 200 words) A wind power system differs from a conventional power system. In a conventional power plant, the operator can control the plant's output. The output of a wind farm cannot be controlled because the output fluctuates with the wind. In this paper, we investigate the power-system interaction resulting from power variations at wind farms using steady-state analysis.			
14. SUBJECT TERMS wind turbine; power system; wind farm; renewable energy; stability; voltage fluctuation; capacitor compensation; induction generator; reactive power compensation		15. NUMBER OF PAGES	
		16. PRICE CODE	
17. SECURITY CLASSIFICATION OF REPORT Unclassified	18. SECURITY CLASSIFICATION OF THIS PAGE Unclassified	19. SECURITY CLASSIFICATION OF ABSTRACT Unclassified	20. LIMITATION OF ABSTRACT UL